# Journal Pre-proof


Climate change-driven aridity threatens vegetation vigor in the Brazilian semiarid region

Lucas Augusto Pereira da Silva, Cristiano Marcelo Pereira de Souza, Edson Eyji Sano, Taya Cristo Parreiras, Édson Luis Bolfe, Bartolomeu Israel Souza, Ramon Santos Souza, Marcos Esdras Leite, Mário Marcos Espírito-Santo, Carolina Cabral das Chagas-Reis, Ivanildo Costa da Silva, João Paulo Sena-Souza, Claudionor Ribeiro da Silva

PII: S2352-9385(26)00105-9

DOI: https://doi.org/10.1016/j.rsase.2026.101972

Reference: RSASE 101972

To appear in: *Remote Sensing Applications: Society and Environment*

Received Date: 22 October 2025

Revised Date: 14 February 2026

Accepted Date: 11 March 2026

Please cite this article as: Pereira da Silva, L.A., Pereira de Souza, C.M., Sano, E.E., Parreiras, T.C., Bolfe, É.L., Souza, B.I., Souza, R.S., Leite, M.E., Espírito-Santo, M.M., das Chagas-Reis, C.C., da Silva, I.C., Sena-Souza, J.P., da Silva, C.R., Climate change-driven aridity threatens vegetation vigor in the Brazilian semiarid region, *Remote Sensing Applications: Society and Environment*, https://doi.org/10.1016/j.rsase.2026.101972.

Lucas Augusto Pereira da Silva[1*],
Cristiano Marcelo Pereira de Souza[3]
Edson Eyji Sano[4],
Taya Cristo Parreiras[5, 6],
Édson Luis Bolfe[5,6],
Bartolomeu Israel Souza[7],
Ramon Santos Souza[7],
Marcos Esdras Leite[8],
Mário Marcos Espírito-Santo[9],
Carolina Cabral das Chagas-Reis[5],
Ivanildo Costa da Silva[1],
João Paulo Sena-Souza[8]
Claudionor Ribeiro da Silva[2]

Geography Department, Campus III – Guarabira, State University of Paraíba (UEPB), Guarabira, PB 58200-000, Brazil[1]

Institute of Geography, Federal University of Uberlândia (UFU), Uberlândia 38408-100, Brazil[2]

Geology Board, Federal University of Vale do São Francisco, Senhor do Bonfim 48970 000, Brazil[3]

Brazilian Agricultural Research Corporation (Embrapa Cerrados), Planaltina 73301-970, Brazil[4]

Institute of Geosciences, State University of Campinas (Unicamp), Campinas 13083-855, Brazil[5]

Brazilian Agricultural Research Corporation (Embrapa Agricultura Digital), Campinas 13083-886, Brazil[6]

Department of Geosciences, Center for Exact and Natural Sciences (CCEN), Federal University of Paraíba (UFPB), João Pessoa 58000-000, Brazil[7]

Department of Geosciences, State University of Montes Claros, Montes Claros 39401-089, Brazil[8]

Department of General Biology, State University of Montes Claros, Montes Claros 39401-089, Brazil[9]

# Climate change-driven aridity threatens vegetation vigor in the Brazilian semiarid region

## Highlights

- Aridity is projected to intensify in the Brazilian semiarid region by the end of the 21st century.
- The Random Forest algorithm performed well ($R^2$ = 0.93, RMSE = 0.02, and MAE = 0.02) in mapping vegetative vigor.
- Increased aridity will induce a decrease of up to 3.58% in vegetative vigor in the Brazilian Semi-arid region.
- Savanna formations are projected to show greening trends in the coming decades (+ 0.78% increase in NDVI).

**Abstract**: Aridification driven by future climate change is expected to significantly change vegetation vigor in global drylands. However, its impacts on the Brazilian semiarid region, one of the world most populous and biodiverse drylands, remains poorly understood. In this study, we employed the Random Forest (RF) model trained with historical edaphoclimatic data to predict changes in vegetation vigor under future climatic scenarios (2061–2080), defined by the Shared Socioeconomic Pathways (SSPs), including an optimistic scenario (SSP1-2.6) and a pessimistic scenario (SSP5-8.5). Model performance was satisfactorily, with the Holdout Test exhibiting $R^2$ = 0.93, RMSE = 0.02, and MAE = 0.02. Seasonal forests are projected to face a decline in greenness (SSP1-2.6 = down to −3.23% and SSP5-8.5 = −7.23%). Similarly, ombrophilous forests are expected to lose between -0.72% and -6.04% in vegetative vigor in the optimistic and pessimistic scenarios, respectively. Despite its natural adaptation to water deficit conditions, the Caatinga biome is also expected to show a significant decrease in vegetation vigor (–2.90% to −3.40%). Ecotonal zones are also projected to lose vegetative vigor (–2.08% to −4.31%). In contrast, savanna formations are expected to undergo a greening trend (+0.78%). Our results provide valuable insights for environmental planning and management, highlighting the most vulnerable vegetation types to future climate-induced aridification.

**Keywords**: Drylands; Random Forest; Greening; Browning; Normalized Difference Vegetation Index.

## 1. Introduction

Drylands cover 41% of the Earth's surface and host more than 38% of the world's population (Huang et al., 2020). These areas contain important vegetation domains that provide crucial ecosystem services and significantly influence socioeconomic systems. Despite their importance, dryland ecosystems are highly sensitive to climate change and rising atmospheric carbon dioxide ($CO_2$) concentrations (Lu et al., 2025). Climate change, especially through increasing aridification, contributes to a decline in vegetation productivity, a phenomenon known as browning. In contrast, increasing $CO_2$ levels can stimulate plant growth, leading to a process known as greening (Piao et al., 2020). Both processes alter the natural dynamics of vegetation, with drylands being disproportionately affected. Model-based studies suggest that most drylands have undergone intense greening in recent decades, partially mitigating water deficiency (Zhang et al., 2024). However, in some areas, the impacts of aridification outperform the benefits of $CO_2$ fertilization, resulting in vegetation browning (Zhang et al., 2024).

In the Brazilian semiarid region (BSR), one of the most populated and biodiverse drylands in the world (Vieira et al., 2015), recent studies have shown a trend toward increasing aridification, followed by progressive browning of vegetation (Pereira et al., 2024). While these historical patterns are relatively well documented, the potential impacts of future aridity on BSR vegetation under climate change conditions remain insufficiently explored. This knowledge gap is especially concerning given the BSR´s high ecological diversity, which includes xerophilous vegetation of the semiarid Caatinga biome, tropical savannas of the Cerrado biome, and both humid and dry tropical forests within the Atlantic Forest biome. These biomes play important roles on a global scale, contributing to variability in primary productivity, water cycling, and the

regulation of atmospheric heat fluxes (Teixeira et al., 2023). At the regional level, BSR vegetation is also vital for supporting local livelihoods and food security of traditional communities.

To address this knowledge gap, consistent and spatially explicit monitoring approaches are needed to capture vegetation dynamics across large and heterogeneous landscapes. Remote sensing, particularly through vegetation indices such as the Normalized Difference Vegetation Index (NDVI), offers a powerful tool for assessing spatiotemporal patterns in vegetation vigor. NDVI captures variations in leaf area and chlorophyll content, making it effective for detecting variations in vegetation vigor under increasing aridity (Higgins et al., 2023). Beyond climate factors, pedological and topographic attributes also have considerable influence on vegetation greenness (Teng et al., 2023). Therefore, integrating edaphoclimatic data is essential for understanding vegetation responses to future climate changes, especially in diverse environments such as the BSR, where complex interactions among soil properties, microclimates, and vegetation types result in highly heterogeneous patterns of vegetative response.

The relationship between edaphoclimatic conditions and vegetation vigor is complex, requiring methodological approaches capable of capturing these multifactorial and often non-linear interactions (Teng et al., 2023). Traditional statistical methods frequently fall short in modeling such multidimensional relationships, especially when integrating diverse environmental variables at large spatial scales. In this context, machine learning offers a powerful alternative, enabling the joint analysis of multiple environmental attributes. Among these approaches, the Random Forest (RF) algorithm has become one of the most widely used tools for vegetation modeling due to its statistical robustness and high predictive performance (Afshari et al., 2025). RF employs a bootstrap aggregation (bagging) approach, incorporating randomness in the selection of training data to reduce overfitting and produce efficient predictions (Liaw and Wiener, 2002).

In this study, we apply the RF algorithm to assess how vegetation vigor in the BSR may respond to intensified aridity under future climate scenarios (2061–2080), based on the Shared Socioeconomic Pathways SSP1-2.6 and SSP5-8.5. We tested the hypothesis that increasing aridity will lead to a decline in vegetation vigor, i.e., browning, over the BSR vegetation in the coming decades. To the best of our knowledge, this is the first study specifically designed to assess how projected aridification will affect vegetation vigor across different biomes covering the BSR. The results of this study will provide a solid scientific foundation to support the formulation and refinement of public policy instruments aimed at the sustainable management of vegetation. These include the establishment of ecological corridors, environmental zoning, and conservation units.

## 2. Materials and Methods

### 2.1. Study area

The study area is located in the northeastern portion of Brazil, between latitudes 0° and 20° S (Figure 1). The BSR is strongly influenced by high atmospheric circulation patterns associated with the Hadley and Walker cells, which generate persistent high-pressure zones over the region (Reboita et al., 2016). These systems are mainly responsible for the region´s semi-arid characteristics, especially the predominance of the BSh climate type in the central portion. This climate is defined by annual temperatures above 18 °C and average annual precipitation ranging from 250 mm to 750 mm (Figure 1a). However, the BSR also includes areas with more humid climates (As, Cwa, and Cwb), especially in the eastern part, which is influenced by moist air masses that originate from the South Atlantic Ocean. In contrast, the western part is characterized by a seasonal tropical climate typical of the Cerrado biome, with two well-defined dry and wet seasons.

The diverse climatic conditions over the BSR have provided a wide variety of landscapes (Figures 1b–g). In the drier areas, physical weathering processes have been responsible for the surface flattening, resulting in extensive depressions with elevations ranging from 350 m to 540 m. These areas are typically associated with shallow soils with low water storage capacity (Figures 1b–d). Such environmental conditions have favored the establishment of the Caatinga biome, characterized by xerophilous vegetation, composed essentially of thorny and deciduous forests adapted to arid conditions (Araújo Filho et al., 2023).

In contrast, the western and eastern zones of the BSR, influenced by more humid conditions and dominated by chemical weathering, are characterized by the presence of plateaus and uplands, where deep, well-drained soils are prevalent. These environments include the Cerrado biome (tropical savanna), which is

distinguished by a mosaic of grasses, shrubs, and sparsely distributed, low-height trees (Ribeiro and Walter, 2008), as well as the Atlantic Forest biome, which encompasses both humid and seasonal forest ecosystems (Moro et al., 2024). Humid forests are composed mainly of broad-leaved, evergreen tree species, while seasonal forests are classified as deciduous or semi-deciduous. These forests shed their leaves during dry periods as an adaptive strategy to avoid excessive water loss through evapotranspiration.

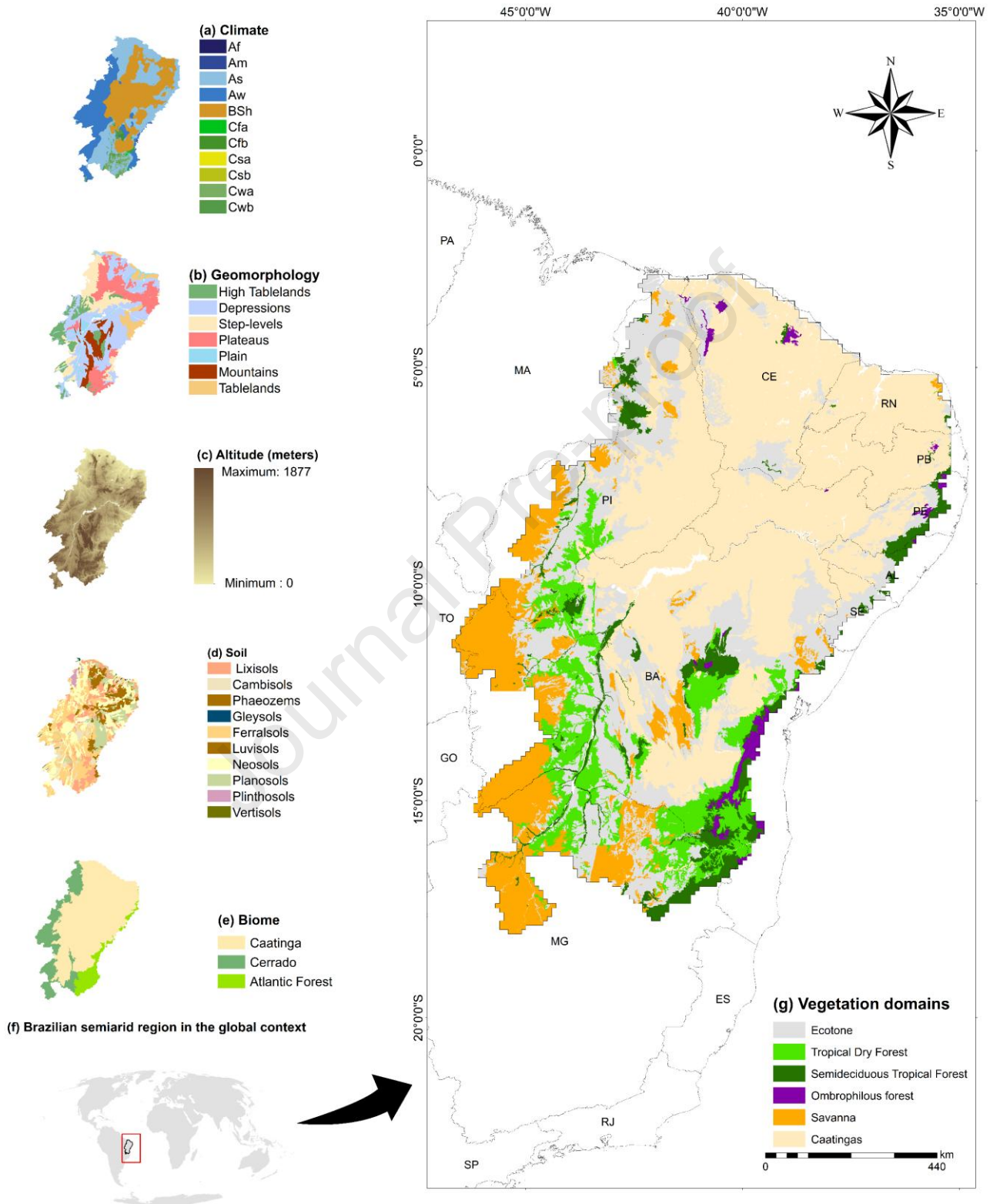


**Fig. 1.** Location and characterization of the study area. (a) Brazilian semiarid region (BSR) in the global context; (b) Climate classification based on Alvares et al. (2013); (c) Geomorphology; (d) Altitude; (e) Soils; (f) Biomes; and (g) Vegetation present in the BSR.

## 2.2. Methodological approach

This study involved the following steps: obtaining the dependent variable (NDVI); assembling a database of environmental covariates; collecting the sample dataset; training and validating the RF algorithm; predicting vegetation vigor under historical and future climate scenarios; and performing statistical analyses (Figure 2).

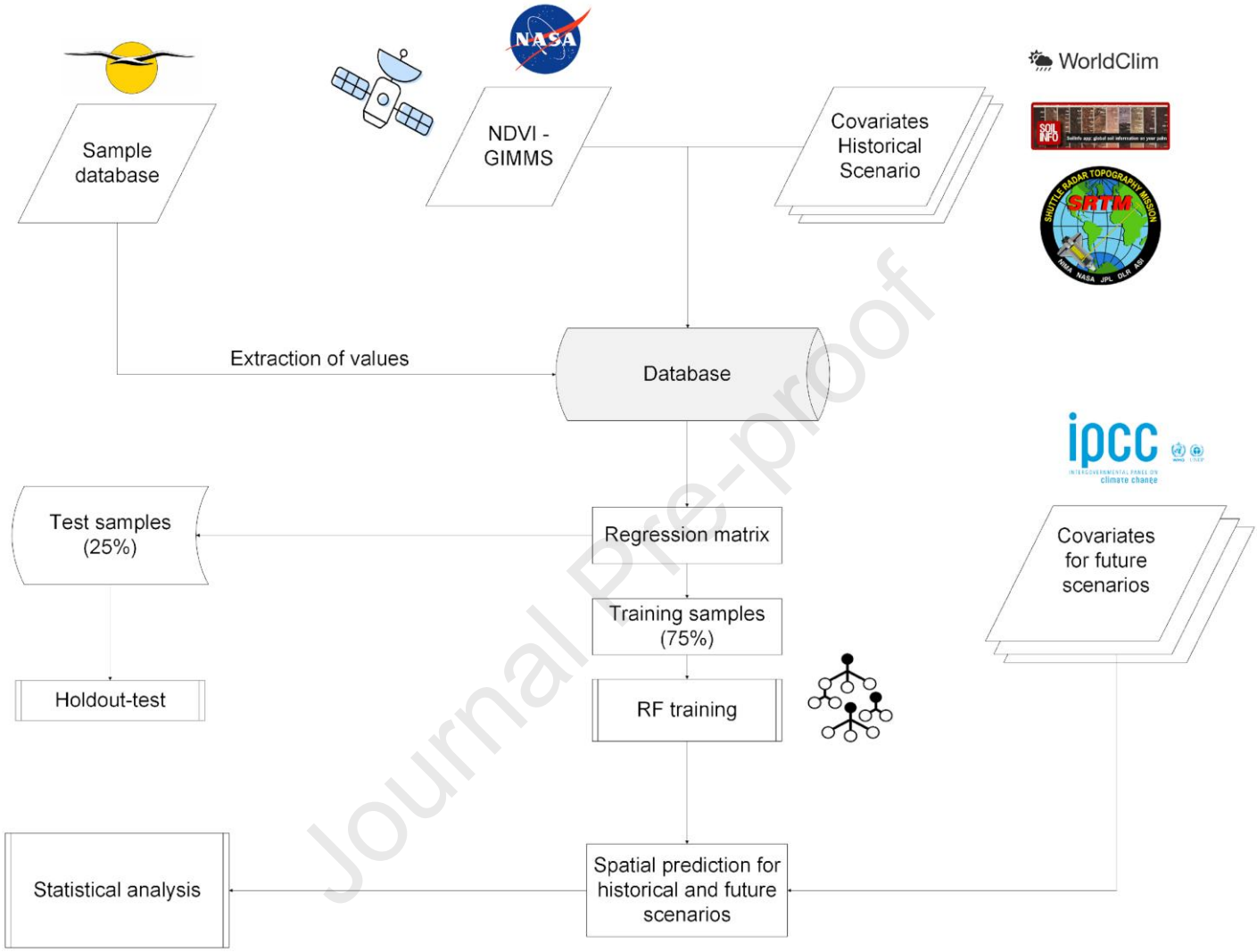


**Fig. 2.** Flowchart of the methodological steps followed in the study. NDVI: Normalized Difference Vegetation Index; GIMMS: Global Inventory Modeling and Mapping System; and RF: Random Forest.

## 2.3. NDVI product

To represent vegetation vigor, we used the NDVI derived from the Global Inventory Modeling and Mapping System (GIMMS NDVI3g), accessed through the Google Earth Engine (GEE) platform. This product is based on observations acquired by the Advanced Very High-Resolution Radiometer (AVHRR) sensors onboard the National Oceanic and Atmospheric Administration (NOAA) satellites. The GIMMS NDVI is based on a robust calibration and quality control process, including corrections for zenith angle bias and atmospheric disturbances caused by aerosols, volcanic eruptions, and cloud cover (Ma et al., 2021). As an additional quality control step, we applied a water mask to exclude negative NDVI values typically associated with water bodies. The dataset provides annual NDVI composites at a spatial resolution of 9.26 km. To ensure compatibility with other spatial databases, we resampled the GIMMS NDVI data to a 10 km resolution using a bilinear interpolation method.

Considering the 15-day temporal resolution of the GIMMS dataset, we obtained approximately 480 NDVI images for the period from 1981 to 2000 and generated a median composite product. We selected the median because it is a measure of central tendency measure that is less affected by outliers in time series data. This procedure is especially effective in reducing noise associated with extreme values, which is relevant in semiarid regions where strong climatic seasonality often results in NDVI extreme values. Although the seasonal dynamics of NDVI are crucial for capturing extreme weather events (e.g., droughts and moisture pulses), the lack of seasonal climate projections for future scenarios hinders this type of analysis. In general, studies focusing on seasonal variability are restricted to historical and present-day contexts (Pereira et al., 2024). Therefore, following previous approaches, we adopted static NDVI data representative of the historical baseline period (Nguyen et al., 2023; Teng et al., 2023).

## 2.4. Environmental covariates database

We used five environmental covariates related to climate, soil properties, and elevation to model vegetation vigor (Table 1). To characterize climate conditions, we employed an aridity index (AI), calculated as the ratio between mean annual temperature (Bio01) and annual precipitation (Bio12), for both the historical (1970–2000) and future (2061–2080) scenarios. We recognize that the AI is commonly calculated from the ratio between potential evapotranspiration and precipitation, as it directly represents the ecological stress of vegetation. However, this approach requires the inclusion of a series of climatic data, such as solar radiation, wind speed, relative humidity, and maximum and minimum temperature. This becomes a limiting factor for the BSR, as the region has a low spatial density of meteorological stations with incomplete historical series. Therefore, the Bio01/Bio12 ratio emerges as a practical alternative due to the limited availability of meteorological data in the BSR. Additionally, studies suggest that air temperature and precipitation are acceptable methods for calculating aridity conditions (Croitoru et l., 2013; Quan et al., 2013; Nyamtseren et al., 2018; Pereira et al., 2024). In this formulation, lower AI values indicate wetter conditions, while higher values reflect drier environments. We obtained the climatic variables Bio01 and Bio12 from the WorldClim 2.1 database (Fick and Hijmans, 2017).

**Table 1.** Covariates used for spatial prediction of vegetative vigor (NDVI).

| Covariates | Abbreviation | Resolution (meters) | Period |
|---|---|---|---|
| Aridity index | AI | 10,000 | Historical and Future |
| Cation exchange capacity | CEC | 250 | Historical |
| Soil organic carbon | SOC | 250 | Historical |
| Clay content | - | 250 | Historical |
| Digital elevation model | DEM | 30 | Historical |
| Deforestation | DEF | 30 | Historical |

Future climate data were derived from general circulation models (GCMs) developed under the Coupled Model Intercomparison Project (CMIP6), based on the Shared Socioeconomic Pathways (SSPs) (IPCC, 2021). These models were calibrated according to different radiative forcing levels, expressed in watts per square meter (W $m^{-2}$) and classified as SSP1-2.6, SSP2-4.5, SSP3-7.0, and SSP5-8.5. The intensification of radiative forcing is directly linked to rising atmospheric $CO_2$ concentrations, which drive increases in global temperature (IPCC, 2021). This relationship between temperature rise and $CO_2$ concentration is referred to as Equilibrium Climate Sensitivity (ECS). ECS is a metric used to describe the sensitivity of GCMs in predicting climate change.

Previous research suggests that ECS values exceeding 5 °C are likely to result in overestimated climate projections and may not reflect plausible climate responses (Hausfather et al., 2022). CMPI6 GCMs

with ESC values above this threshold are often referred to as "hot models" (Hausfather et al., 2022). To reduce the risk of unrealistic projections and overestimation of future climate impacts, we considered only GCMs with ECS values below 5 °C for this study (Table 2). It is worth noting that excluding models with ESC > 5° makes our analysis conservative, as this procedure may lead to an underestimation of extreme aridity values.

**Table 2.** Models used to derive climate covariates. The ensemble model was created from this set of General Circulation Models (GCMs).

| Model | Foundation | Spatial resolution* |
|---|---|---|
| CMCC-ESM2 | Euro-Mediterranean Centre on Climate Change | 192 × 144 |
| GISS-E2-1-G | National Aeronautics and Space Administration | 144 × 90 |
| INM-CM5-0 | Institute for Numerical Mathematics and Russian Academy of Science | 180 × 120 |
| IPSL-CM6A-LR | Institut Pierre-Simon Laplace | 250 × 126 |
| MIROC6 | Japan Agency for Marine-Earth Science and Technology | 141 × 141 |
| MPI-ESM1-2-HR | PRIMAVERA Project data from the Max Planck Institute for Meteorology | 384 × 192 |
| MRI-ESM2-0 | Meteorological Research Institute | 113 × 113 |

* These values refer to the native spatial resolution of the GCMs. However, the datasets obtained from the WorldClim platform are statistically downscaled and corrected for bias to a spatial resolution of 10 km. Therefore, despite differences in their original native resolutions, all GCMs used in this study were harmonized to a common spatial resolution of 10 km.

GCMs were obtained for two contrasting SSP1-2.6 (optimistic) and SSP5-8.5 (pessimistic) scenarios. The optimistic scenario projects a global temperature increase between 1.5 °C and 2 °C, aligning with the targets set by the Paris Agreement. Under this scenario, a sustainable path of preservation of natural resources is expected. In contrast, the pessimistic scenario projects a global temperature increase of up to 4 °C in the coming decades, especially driven by high $CO_2$ emissions and significant changes in land use and land cover dynamics (IPCC, 2021). Considering the variations in the formulation of the GCMs, we created an ensemble model for the AI by calculating the arithmetic means of the outputs from the seven selected models. This procedure has been adopted in previous studies to reduce uncertainties in climate projections (Teng et al., 2023).

We obtained the soil database from the SoilGrids platform (Poggio et al., 2021), consisting of three physical and chemical attributes measured at a depth of 0–5 cm: soil organic carbon (SOC), cation exchange capacity (CEC), and clay content. These covariates are critical for assessing vegetation vigor, as they directly influence soil structure, water holding capacity, and the availability of nutrients necessary for plant growth (Araújo Filho et al., 2023; Teng et al., 2023). In addition, these attributes represent the most prominent soil characteristics found in the BSR (Araújo Filho et al., 2023). Previous studies carried out in the region have shown the importance of incorporating soil properties into vegetation modeling to improve predictive accuracy (Oliveira et al., 2021; Pereira et al., 2024).

We obtained the elevation data from the Shuttle Radar Topography Mission (SRTM) (van Zyl, 2001). This covariate is frequently used in vegetation vigor assessments because of its role in stratifying vegetation density along topographic gradients. This influence is basically driven by its impact on microclimate conditions, especially wind speed, air temperature, and humidity, as well as on hydrological processes, including surface runoff and groundwater dynamics (Teng et al., 2023).

Additionally, we included a deforestation covariate derived from the MapBiomas Project (MapBiomas, 2023). This product consists of a categorical variable obtained through supervised classification based on remote sensing data and represents deforested and non-deforested areas in the BSR for the accumulated period of 1986–2023. We included this anthropogenic proxy because, in combination with edaphoclimatic factors, it helps understand the spatial patterns of vegetative vigor (Liu et al., 2022). Due to the lack of future deforestation projections for the BSR, we assumed that the accumulated deforestation pattern observed between 1986 and 2023 will remain constant in the coming decades. Finally, the soil, DEM, and deforestation covariates were resampled to a 10 km resolution using the bilinear interpolation to ensure consistency over all spatial layers.

## 2.5. Sample database

We compiled a dataset of 984 samples representing the six most dominant vegetation domains in the BSR: Caatinga (*n* = 328), Ecotone (*n* = 265), Tropical Dry Forest (TDF; *n* = 96), Semideciduous Tropical Forest (SDTF; *n* = 37), Ombrophilous Forest (*n* = 79), and Savanna (*n* = 179) (Figure 3; Table 3). We obtained these samples from the RADAMBRASIL project, available through the Environmental Information Bank (BDia) of the Brazilian Institute of Geography and Statistics (IBGE) (IBGE, 2023). The sampling points were collected during field campaigns conducted by this project between 1973 and 1982. We selected this database because it is temporally aligned with the historical environmental covariates used in this study and is considered as the official source of vegetation mapping in Brazil.

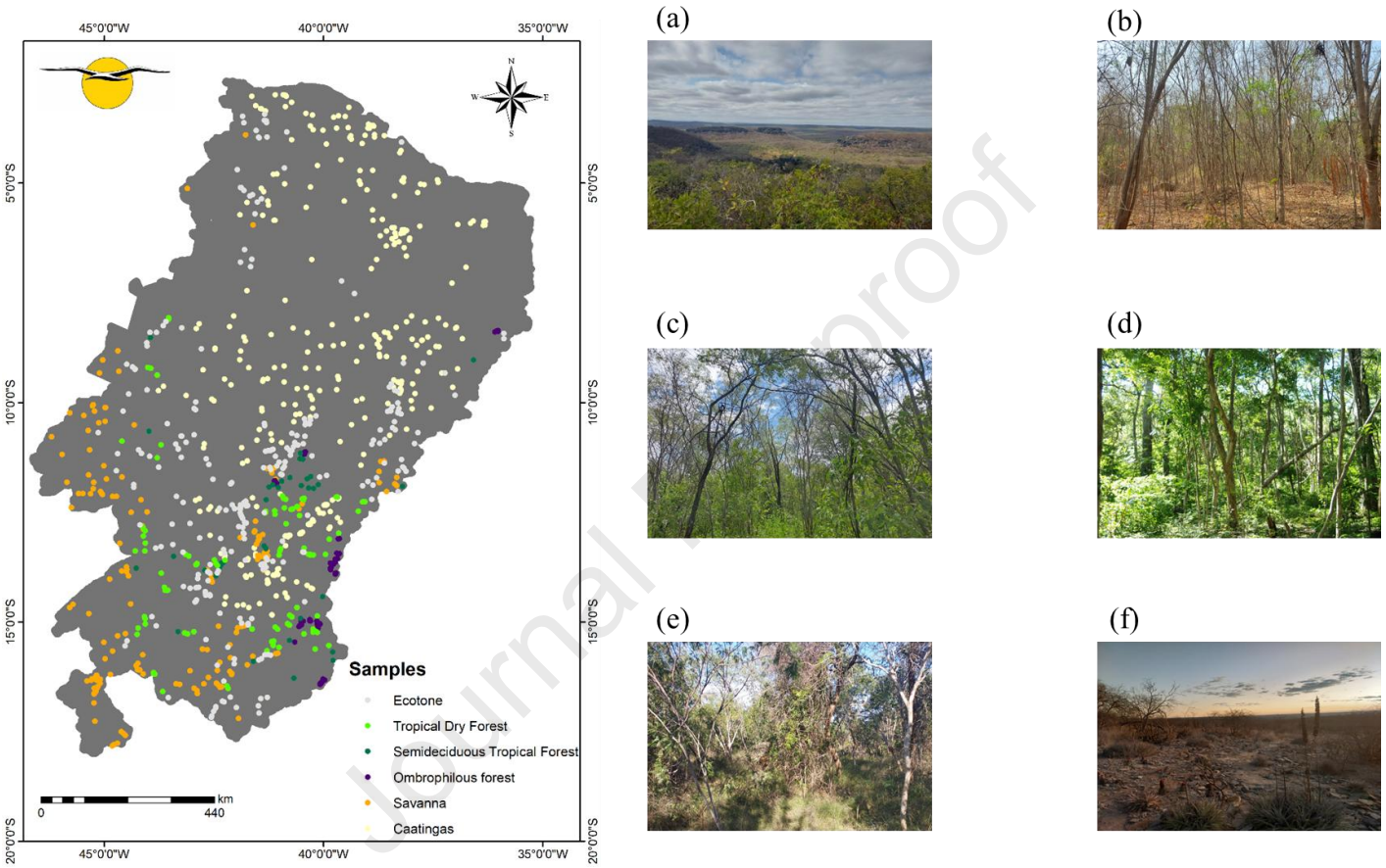


**Fig. 3**. Representative samples from the six major vegetation domains of the Brazilian semiarid region, according to the RADAMBRASIL project. (a) Ecotone; (b) Tropical Dry Forest; (c) Semideciduous Tropical Forest; (d) Ombrophilous Forest; (e) Savanna; (f) Caatinga.

**Table 3**. Number of samples and description of vegetation domains.

| Vegetation Domain | Samples | Description |
|---|---|---|
| Caatinga | 328 | Characterized by shrubs and arboreous strata. It develops over shallow soils derived from crystalline rocks and is well-adapted to prolonged droughts lasting up to eight months. |
| Ecotone | 265 | Transition zone between two or more vegetation domains, characterized by ecological tension and active interaction among coexisting plant communities. |
| Tropical Dry Forest | 96 | Forest domain showing adaptative mechanisms, such as the loss of up to 90% of its leaves to reduce physiological stress during prolonged drought periods. |

| | | |
|---|---|---|
| Semideciduous Tropical Forest | 37 | Phytophysiognomy adapted to seasonal water deficiency, with leaf loss of up to 50% during the dry season. |
| Ombrophilous Forest | 79 | Dense forest formations with well-developed shrub and arboreal strata, highly dependent on abundant water availability and generally not subject to annual water deficits. |
| Savanna | 179 | Predominance of savanna formations comprising trees, shrubs, and herbaceous strata, marked by pronounced climatic seasonality with well-defined dry and wet seasons. |

## 2.6. Training and validation

Vegetation samples were used to create a regression matrix containing NDVI values and their corresponding environmental covariates for the historical scenario. To assess multicollinearity among predictors, we applied the *findCorrelation()* function from the *Caret* package in R (version 4.3.2) (Kuhn et al., 2020), adjusted by the Pearson correlation method with a cut-off threshold of 0.70. The analysis confirmed that no covariates presented high collinearity (Supplementary Figure S1). Subsequently, we partitioned the dataset into training (75%) and validation (25%) subsets using the *split()* function.

We used the RF algorithm to predict vegetation vigor in the BSR. We chose RF due to its strong capacity to model complex, non-linear relationships between vegetation vigor and environmental variables. This potential is associated with its bootstrap-based approach, which builds multiple decision trees using subsets of predictors during the training phase (Liaw and Wiener, 2002). Each tree generates an individual prediction, and the final prediction is obtained by averaging the results of all trees in the forest, thereby improving robustness and reducing overfitting (Liaw and Wiener, 2002).

Using the framework provided by the *Caret* package, we trained the RF model with 75% of the available samples. The training process was based on 10-fold cross-validation method with five repetitions, a method that partitions the data into 10 subsets and performs five rounds of training to ensure model robustness. Model performance during training was evaluated using the following statistical performance indicators: R-squared ($R^2$), root mean squared error (RMSE) and mean absolute error (MAE). Hyperparameters tuned during cross-validation included the number of covariates selected at each split (*mtry*) and the number of trees in the forest (*ntree*). To identify the most influential covariates for prediction, we used the *varImp()* function, which ranks covariates based on their contribution to model accuracy. We used linear regressions and partial dependence plots created with the *pdp* and *ggplot2* packages (Brunson, 2020; Greenwell, 2017) to assess the relationship between the most important covariates and NDVI. Finally, we evaluated the model's performance using the holdout-test method with the remaining 25% of the samples. Model accuracy was assessed based on $R^2$, RMSE, and MAE, calculated via the *Metrics* package (Hamner and Frasco, 2012).

## 2.7. Spatial prediction

Using the RF model trained with the AI, soil attributes, and elevation data, we employed the *predict()* function from the *raster* package (Hijmans et al., 2015) to spatialize vegetation vigor for the historical scenario (1970–2000). For future scenarios, we replaced the historical AI layer with the ensemble model based on the optimistic and pessimistic IPCC scenarios. We assume that soil properties and elevation will remain constant in the coming decades, especially due to the lack of cartographic databases that account for future pedogenetic and morphometric changes. However, this assumption represents a methodological simplification that may not fully capture the effects of intensified land use and land cover practices on soils conditions, potentially leading to an overestimation of NDVI values in future scenarios.

Cumulative deforestation for the period 1986–2023 was treated as constant due to the lack of future projections for the BSR. This assumption may make our approach conservative, since deforestation rates in the BSR have shown a linear increasing trend in recent decades, which could persist under future conditions.

## 2.8. Statistical analysis

We performed a comparative analysis to assess the percentage change in vegetation vigor between the historical and future scenarios for the BSR. We applied the following equation (Eq, 1):

$$\Delta NDVI\% = \left(\frac{NDVI_{Fs} - NDVI_{Hs}}{NDVI_{Hs}}\right) \times 100 \quad (1)$$

Where: *ΔNDVI%* represents the percentage difference in vigor between the scenarios, *NDVI_Fs* is the predicted vigor for both the optimistic and pessimistic scenarios, and *NDVI_Hs* is the vigor for the historical scenario.

Next, we applied the Kruskal-Wallis test, followed by the Dunn test, to assess significant differences in vegetation vigor among the vegetation domains under climate change scenarios (Kruskal and Wallis, 1952; Dunn, 1964). We considered the Z-score and a level of significance of 5% ($p < 0.05$). The Z-score represents the standardized difference between NDVI values of the vegetation domains when comparing the historical baseline with future scenarios. Higher absolute Z-score values indicate a greater likelihood of statistically significant differences ($p < 0.05$). All analysis was performed using the FSA package (Ogle et al., 2023).

## 3. Results

### 3.1. Random Forest performance and importance of covariates

The RF model showed good performance in mapping NDVI for the historical baseline (1970–2000), with holdout test results showing an $R^2$ of 0.93, RMSE of 0.02, and MAE of 0.01 (Figure 4). Cross-validation further confirmed the robustness and reliability of the model. The selected covariates explained 92% of the variation in NDVI. Among these covariates, the AI showed to be the most influential variable (overall = 100%), followed by SOC (52.46%), DEM (14.66%), and CEC (11.15%), while Clay and deforestation showed the importance of less than 10%. These covariates showed statistically significant relationships with NDVI, characterized by non-linear marginal responses as revealed by the partial dependence plots (Figures 5 and 6). Higher vegetation vigor in the BSR was predominantly observed in more humid zones (AI ~0.020 – 0.025 °C $mm^{-1}$), higher elevations (800 – 900 m), and in soils rich in organic carbon (~450 dg/kg) and with lower CEC (90 – 130 cmolc $kg^{-1}$). In contrast, areas with reduced vegetation vigor were typically located in more arid environments (AI ~ 0.045–0.070 °C $mm^{-1}$), at lower elevations (< ~350 m), and in soils characterized by high cation retention capacity (> ~230 cmolc $kg^{-1}$) and low organic carbon content (< ~120 dg $kg^{-1}$) (Figure 6).

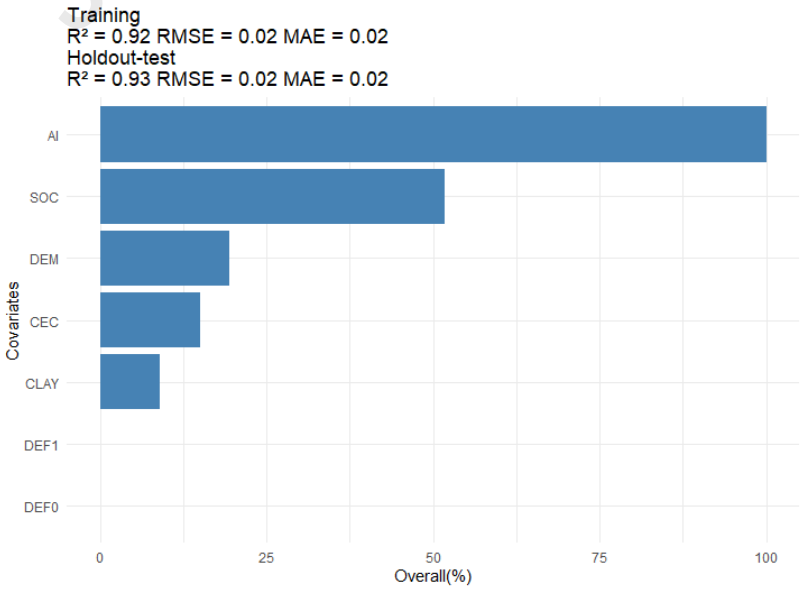


**Fig. 4**. Performance metrics of the Random Forest model for the training and holdout test datasets, along with the relative importance of explanatory variables expressed as Overall (%). Model performance was evaluated using the coefficient of determination ($R^2$), root mean squared error (RMSE), and mean absolute error (MAE). AI: Aridity Index; SOC: Soil Organic

Carbon; DEM: Digital Elevation Model; CEC: Cation Exchange Capacity; DEF1: deforestation; DEF0: no-deforestation. The RF model was tuned with the following hyperparameters: mtry = 2; and ntree = 500.

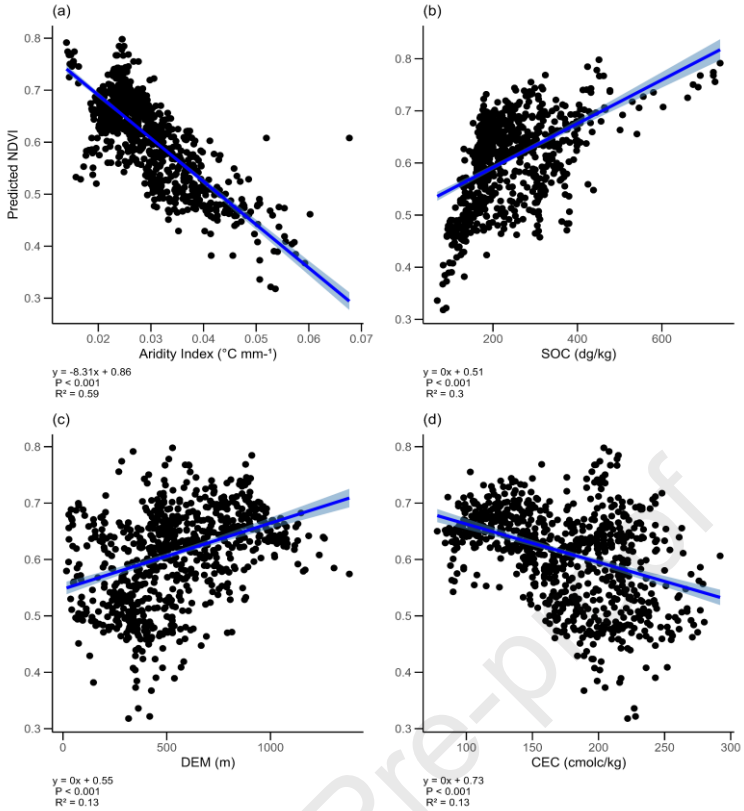


**Fig. 5**. Linear relationships between the most influential covariates and NDVI, including the corresponding coefficients of determination ($R^2$) and statistical significance levels (p-values).

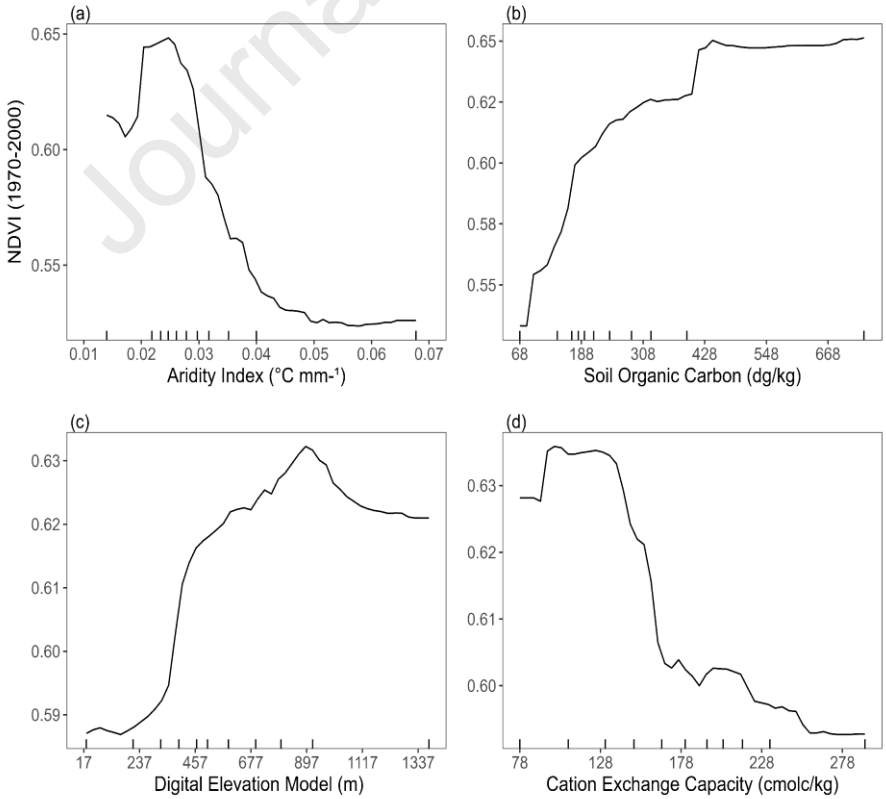


**Fig. 6**. Partial dependence plots depicting the influence of key covariates on NDVI patterns, as modeled by the Random Forest algorithm.

### 3.2. Aridity Index (AI) projections

Our results suggest that the BSR will experience increasing aridity by the end of the century (Figure 7). For the historical baseline (1970–2000), the mean AI was 0.031 °C $mm^{-1}$. Ensemble modeling suggests that this value will increase by 9.68% under the optimistic climate scenario and by 19.35% under the most pessimistic scenario.

During the historical period, the driest regions (AI > 0.045 °C $mm^{-1}$) accounted for 8.03% of the BSR (96,400 km²), mainly located in the central Bahia and Pernambuco, as well as in northeastern Paraíba and Ceará, areas largely overlapping the Caatinga biome. Under the most pessimistic scenario, these arid lands are projected to expand up to 21% of the BSR (255,600 km²). Even under the optimistic scenario, an expansion of approximately 75,900 km² in arid land is expected.

Historically humid lands (AI < 0.023 °C $mm^{-1}$) covered 16% of the BSR (194,100 km²), mainly concentrated along the eastern margin in the Atlantic Forest biome and in portions of the western sector within the Cerrado biome. Under the most pessimistic climate projections, the extent of these humid areas is expected to decrease dramatically, covering only 7% of the BSR.

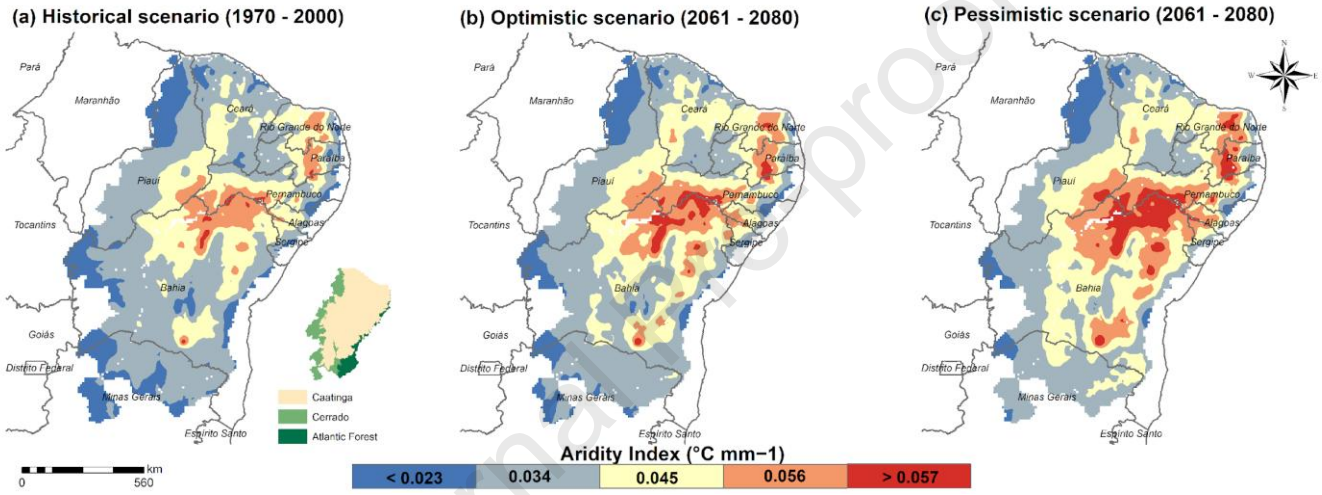


**Fig. 7**. Projected aridity patterns in the Brazilian semiarid region derived from an ensemble of five General Circulation Models. Maps represent the historical baseline (a), the optimistic future scenario (b), and the pessimistic future scenario (c).

### 3.3. Vegetation vigor (NDVI) response to aridification under future scenarios

Climate change is projected to significantly alter vegetation vigor (NDVI) across the BSR in the coming decades (Figure 8). Under the historical climate scenario, the mean NDVI was 0.586. However, projections based on future IPCC scenarios indicate a potential decline of up to 3.58% in the regional NDVI. The most pronounced reductions in vegetative vigor (up to -24.61%) are expected in the southeast and eastern regions of the BSR over the Caatinga and Atlantic Forest biomes (Figure 9). In contrast, the southwestern and western regions (in the Cerrado biome) are expected to show increases of up to 16.27% in NDVI.

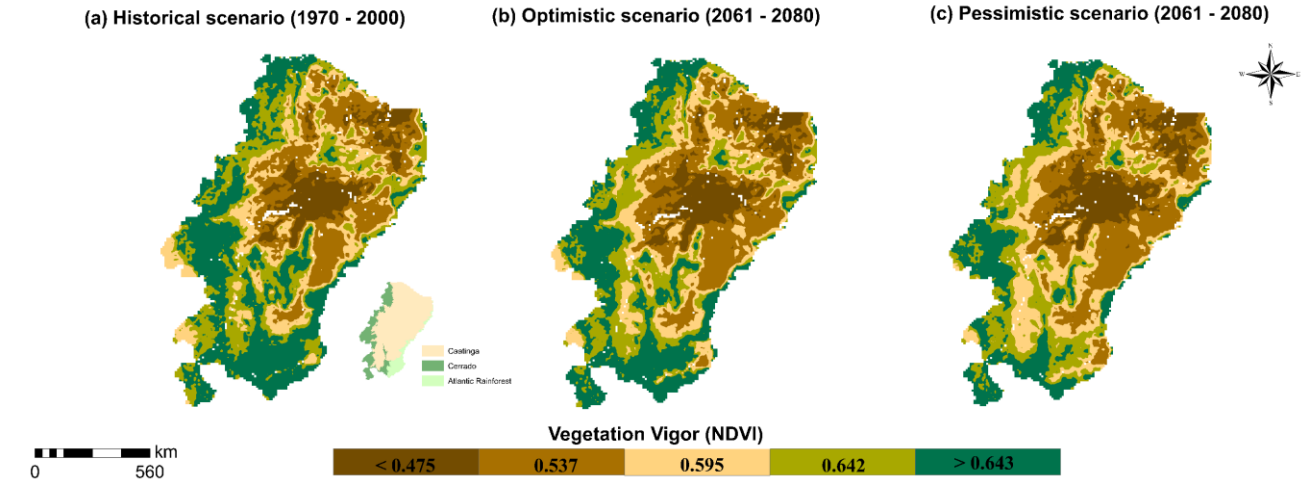


**Fig. 8.** Spatial distribution of vegetation vigor (NDVI) in the Brazilian Semiarid Region under the historical (a), optimistic (b), and pessimistic (c) climate scenarios. The figure also displays the geographical distribution of the region´s major biomes for reference.

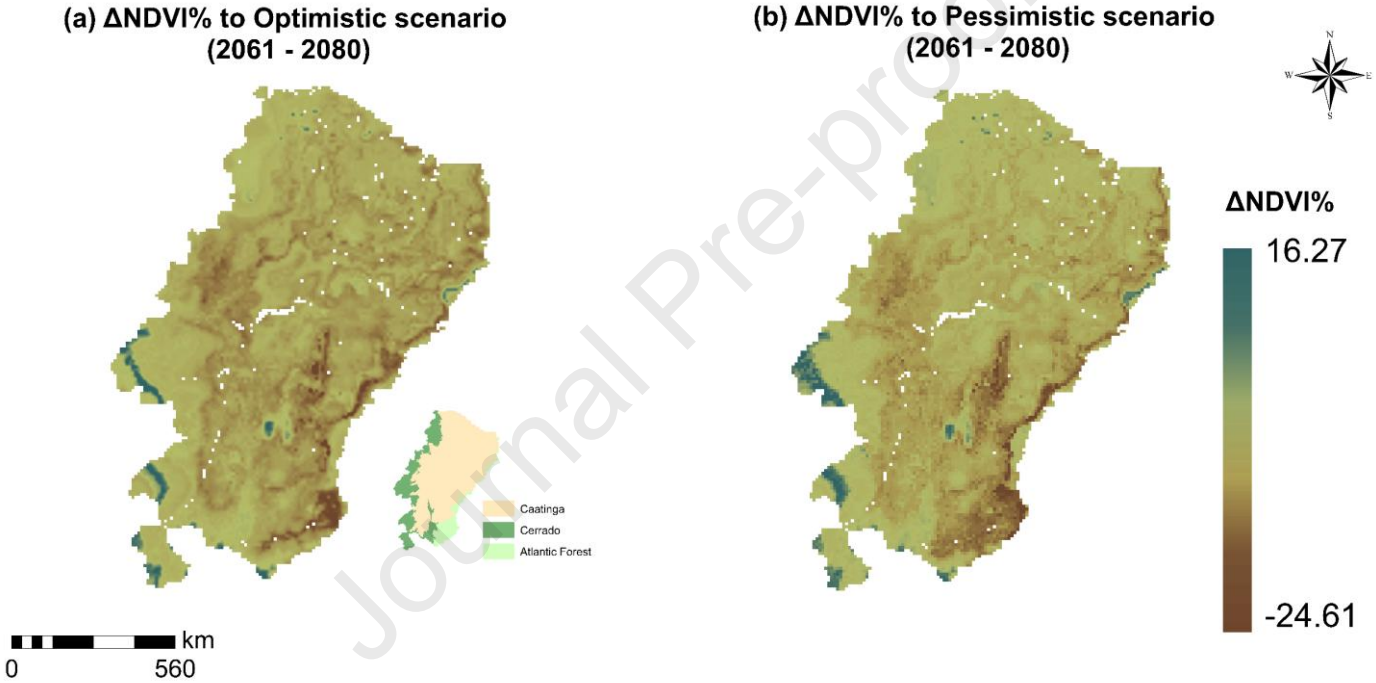


**Fig. 9**. NDVI difference maps for the optimistic (a) and pessimistic (b) future scenarios.

Consistent with broader regional trends, vegetation vigor across the BSR´s major ecological domains are expected to undergo significant changes in the coming decades (Tables 4 and 5). Tropical forests, both ombrophilous and seasonal, are projected to undergo the most intense declines in vegetation vigor due to the increasing aridity (Figure 10). The ombrophilous forest, which is historically adapted to humid conditions (AI = 0.021 °C $mm^{-1}$), presented the highest levels of greenness during the historical period (1970–2000), with a mean NDVI of 0.695. However, under future climate scenarios, projected increases in aridity (from +0.03 °C $mm^{-1}$ to 0.005 °C $mm^{-1}$) are expected to result in a 6.04% reduction in the historical NDVI average.

Seasonal forests, including tropical dry forests (TDF) and subtropical dry forests (STDF), are also expected to experience marked browning under future climate scenarios. In the historical scenario, these forests were in areas with AI values ranging from 0.024 °C $mm^{-1}$ to 0.027 °C $mm^{-1}$, with mean NDVI values of 0.650 for TDF and 0.656 for STDF. With an increase of up to 0.006 °C $mm^{-1}$ in AI, the historical mean NDVI of these forests is projected to decline significantly, with a loss of 7.23% for TDF and 5.49% for STDF.

The Caatinga biome, which is naturally adapted to the most arid conditions in the BSR, showed an AI of 0.037 °C $mm^{-1}$ and the lowest historical mean NDVI of 0.530. According to the IPCC scenarios, an increase of up to 0.006 °C $mm^{-1}$ in AI is projected, which would lead to a decline of up to 3.40% in the historical mean NDVI in the Caatinga biome, despite its adaptation mechanisms to arid conditions.

**Table 4**. Results of the Kruskal-Wallis test followed by Dunn´s post hoc test comparisons between the historical baseline and future climate projections. Positive Z-scores indicate a browning trend, while negative Z-scores suggest a greening trend. P-values < 0.05 indicate statistically significant differences.

| Comparison | Z-score | P.unadj | P.adj |
|---|---|---|---|
| **Caatinga** | | | |
| Historical vs Optimistic | 8.13 | 0.00 | 0.00 |
| Historical vs Pessimistic | 12.77 | 0.00 | 0.00 |
| **Ecotone** | | | |
| Historical vs Optimistic | 7.86 | 0.00 | 0.00 |
| Historical vs Pessimistic | 15.20 | 0.00 | 0.00 |
| **Tropical Dry Forest** | | | |
| Historical vs Optimistic | 8.61 | 0.00 | 0.00 |
| Historical vs Pessimistic | 18.86 | 0.00 | 0.00 |
| **Semi-deciduous Tropical Forest** | | | |
| Historical vs Optimistic | 3.76 | 0.00 | 0.00 |
| Historical vs Pessimistic | 10.57 | 0.00 | 0.00 |
| **Ombrophilous Forest** | | | |
| Historical vs Optimistic | 1.13 | 0.26 | 0.77 |
| Historical vs Pessimistic | 5.16 | 0.00 | 0.00 |
| **Savanna** | | | |
| Historical vs Optimistic | −3.46 | 0.00 | 0.00 |
| Historical vs Pessimistic | −3.90 | 0.00 | 0.00 |

**Table 5.** Mean NDVI and Aridity Index (AI) values for the six vegetation domains in the Brazilian Semiarid Region, considering historical and future optimistic and pessimistic climate scenarios.

| Vegetation | Aridity Index | | | NDVI | | |
|---|---|---|---|---|---|---|
| | Historical | Optimistic | Pessimistic | Historical | Optimistic | Pessimistic |
| Caatinga | 0.037 | 0.040 | 0.043 | 0.530 | 0.519 | 0.512 |

| | | | | | | |
|---|---|---|---|---|---|---|
| Tropical Dry Forest | 0.027 | 0.030 | 0.034 | 0.650 | 0.629 | 0.603 |
| Semi-deciduous Tropical Forest | 0.024 | 0.027 | 0.030 | 0.656 | 0.643 | 0.620 |
| Ecotone | 0.028 | 0.030 | 0.033 | 0.626 | 0.613 | 0.599 |
| Ombrophilous Forest | 0.021 | 0.024 | 0.026 | 0.695 | 0.690 | 0.653 |
| Savanna | 0.022 | 0.024 | 0.026 | 0.637 | 0.642 | 0.642 |

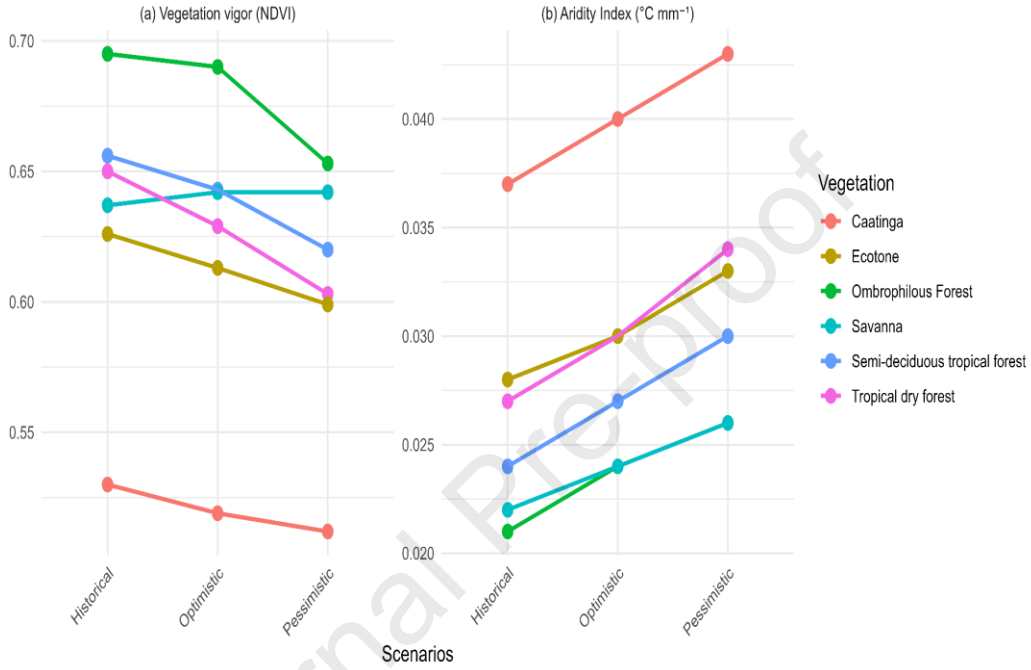


**Fig. 10**. Trends in Aridity index (AI) and vegetative vigor (NDVI) across the vegetation domains in the Brazilian Semiarid Region, comparing the historical baseline with future optimistic and pessimistic climate scenarios.

Surprisingly, regardless of intensification of aridity compared to the historical scenario (AI increase of 0.002 °C $mm^{-1}$ to 0.004 °C $mm^{-1}$), savannas are projected to undergo a significant greening process in the coming decades, with a 0.78% increase in the mean NDVI. This demonstrates the resilience of savanna in response to future climate conditions.

Ecotonal zones in the BSR are projected to experience intensified aridity in the coming decades, with AI increases ranging from 0.003 °C $mm^{-1}$ to 0.005 °C $mm^{-1}$. This intensification of aridity is expected to lead to a browning process, especially in ecotones where Caatinga and tropical forests coexist. In contrast, ecotones areas bordering savanna may exhibit an increase in vegetative vigor. These contrasting patterns highlight the ecological complexity of ecotones and their heterogeneous responses to climate change in semiarid environments.

## 4. Discussion

### 4.1. Impacts of covariates on vegetation vigor

Our NDVI mapping using the RF algorithm, based on a limited set of edaphoclimatic variables, demonstrated a good statistical performance, with $R^2$ = 0.74, MAE = 0.05, and RMSE = 0.04. These results are consistent with those reported in both global and regional vegetation modeling studies using RF and other decision tree-based algorithms (Ma et al., 2025; Teng et al., 2023).

AI emerged as the most influential covariate in explaining the spatial distribution of vegetation vigor in the BSR. Aridity directly reflects surface water availability, which is a critical factor for plant physiological processes (Yang et al., 2025). In more arid areas, limited water availability leads to stomatal closure, reducing photosynthetic activity and, consequently, vegetation vigor (Yang et al., 2025). Conversely, in less arid zones, vegetation tends to maintain better metabolic functioning, therefore, showing high levels of vigor (Liu et al., 2019).

SOC also showed strong explanatory power for variations in vegetation vigor across the BSR. A positive relationship was observed between SOC and NDVI, suggesting that areas with higher SOC concentrations are associated with increased vegetation greenness. In general, this relationship is largely due to the role of organic carbon in improving soil structure, especially through improved aggregate stability and increased water holding capacity, which are beneficial for plant growth (Tisdall and Oades, 1982). Similar findings have been reported in other vegetation modeling studies, which have consistently highlighted the importance of SOC in driving NDVI (Dou et al., 2025).

Elevation also exerted a positive influence on vegetation vigor in the BSR. This result is consistent with previous studies in the region (Pinto et al., 2025), which have shown that denser vegetation typically occurs in areas with higher elevations, such as the 'Brejos de Altitude' within the Atlantic Forest biome. These elevated areas, such as plateaus and mountains, often experience reduced water stress, especially due to lower temperatures and the occurrence of orographic rainfall (Ramos et al., 2020). Such factors contribute to the maintenance of more humid conditions, which help to preserve water availability and, consequently, maintain higher levels of vegetation vigor.

Surprisingly, CEC, often associated with soil fertility, showed a negative relationship with vegetation vigor in the study area. Although this result may initially appear contradictory, it reflects the dynamics of certain soils of the Caatinga biome, especially Luvisols and Vertisols, which develop under conditions of limited rainfall (EMBRAPA, 2018). In these arid conditions, reduced leaching promotes the accumulation of highly reactive clay minerals, leading to elevated CEC values (Araújo Filho et al., 2023). However, persistent water scarcity restricts the effective uptake of nutrients by plants, thereby reducing the productive potential of the environment. As a result, xerophytic vegetation predominates in these areas, composed of drought-adapted, low-stature, sparsely distributed species, resulting in consistently low NDVI values. This pattern reveals the ecological constraints imposed by aridity, even in soils with high chemical fertility.

### 4.2. Impact of intensified aridity on vegetation vigor

Our modeling results suggest that increased aridity could lead to a reduction of around 3.58% in NDVI in the BSR region under future scenarios. Notably, these projected declines are consistent with observed historical trends in the study region. For example, Pereira et al., (2024) reported a 7.4% decrease in vegetation levels over the past 22 years in the BSR region, associated with increased aridity. Similarly, Tomassella et al., (2025) attributed increasing vegetation stress in Brazilian semiarid lands to the amplification of aridification in recent decades.

Consistent with the broader regional trend, our projections indicate a significant decline in tropical and seasonal forest cover in the BSR. Browning of ombrophilous forest is linked to the intensification of aridity and consequently exacerbated water limitation. Under these conditions, ombrophilous forest that are historically adapted to humid environments suffer from increased water demand, which can induce hydraulic failure, consequently decreasing photosynthesis rates and ultimately green levels (Pereira et al., 2024). Additionally, this physiological stress can not only reduce greening, but also lead to changes in species composition, favoring the transition from humid vegetation to deciduous species more tolerant to drought (Aguirre-Gutiérrez et al., 2025), the advance of savannas (Oliveira et al., 2021), and, in more severe cases, result in widespread tree mortality (Robbins et al., 2024). Although seasonal forests are generally considered more resilient to prolonged drought, often showing rapid leaf recovery following dry periods (Stan et al., 2021), our results suggest that even these ecosystems are likely to experience browning in the coming decades. This anticipated decline in vegetation vigor may be attributed to the reduced germination capacity of seasonal forest species under intense water stress, which constrains natural regeneration processes (Dias et al., 2024). Furthermore, the effects of aridification may be worsened by high levels of forest fragmentation and degradation, factors that increase ecosystem vulnerability to climate change (Stan et al., 2024).

Similarly, in the Caatinga, one of the most vulnerable Brazilian biomes due to alarming deforestation rates and advanced land degradation (Franca Rocha et al., 2024), a significant decline in vegetation vigor is projected under future climate change scenarios. This downward trend has already been observed in recent years and is largely associated with ongoing aridification processes in the region (Pereira et al., 2024). Increasing aridity is likely to favor the persistence and expansion of hyperxerophilous species, plants highly adapted to extreme dryness, a factor that may further reduce overall vegetation vigor (Oliveira et al., 2022). Furthermore, consistent with global assessments (Huang et al., 2020), the amplification of aridity is expected to accelerate desertification processes in the BSR, reducing primary productivity in the Caatinga and contributing to widespread browning (D'Odorico et al., 2013). Therefore, although the Caatinga has high water use efficiency (WUE) (Borges et al., 2024), these ecological changes resulting from aridification can promote the expansion of semi-desert ecosystems, potentially leading to substantial biodiversity losses (Oyama and Nobre, 2004). Despite these alarming projections, the xerophilous vegetation of the Caatinga has historically received limited attention in Brazil´s environmental policies. Currently, only 8% of its territory is designated as conservation units, with just 1% under full protection status (Santos et al., 2011). Considering the Caatinga´s high biodiversity, high levels of endemism, and its crucial role in supporting traditional communities (Moro et al., 2024), expanding conservation efforts is imperative to safeguard this unique and increasingly vulnerable biome.

Interestingly, the savanna domain (Cerrado biome) was the only vegetation projected to experience significant greening in the coming decades, even under intensified aridity. This increase in vegetation vigor may be associated with the unique physiological mechanisms of savanna plants and the pedological characteristics of the biome (Ribeiro and Walter, 2008; Pereira et al., 2024). Savanna species possess key drought-tolerance mechanisms, including seasonal leaf shedding to reduce transpiration losses and the development of deep and extensive root systems that enable access to water stored in deeper soil layers during prolonged dry periods (Pereira et al., 2024; Yang et al., 2025). Furthermore, savanna soils are typically deep and well-drained, favoring water retention in subsurface horizons, which enhances plants access to moisture during drought events (Ribeiro and Walter, 2008). The combination of these physiological and edaphic factors may mitigate the effects of aridification, promoting ecosystem resilience under future climate conditions. Additionally, previous research suggests that the greening of savannas may be associated with high concentrations of $CO_2$ in the atmosphere (Scheiter and Higgins, 2009). In this case, high $CO_2$ improves photosynthesis rates and increases efficient water use through partial stomatal closure (Jian et al., 2023), consequently alleviating water restriction, inducing fertilization, which can stimulate plant growth, increase leaf area, and promote higher biomass accumulation (Scheiter and Higgins, 2009).

Ecotonal zones display complex and variable responses in vegetation vigor under future climate change scenarios. In transitions between the Caatinga and tropical forests, a browning trend is expected for the coming decades. This pattern may indicate the encroachment of xerophilous species into more humid forest formations, contributing to a process of xerification (Oliveira et al., 2021). In contrast, ecotonal transitions adjacent to savanna formations are likely to undergo greening in the BSR (Pereira et al., 2024). However, Oliveira et al. (2021) suggested that the expansion of xerophilous species could also extend into savanna-dominated ecotones under increased aridity. Despite this potential shift, the unique physiological adaptations and favorable pedological condtions of savanna ecosystems may buffer the effects of aridification, partially mitigating the climate change impacts and promoting ecosystem resilience.

### 4.3. Uncertainties and future directions

Although our modeling performed well ($R^2 = 0.93$), some limitations need to be acknowledged. The dataset used to model vegetation vigor was relatively limited in scope and specifically designed to reflect the environmental specificities of the BSR. As a result, the selected covariates may not adequately represent the ecological and climate complexities of other regions, potentially restricting the broader applicability of the model. Therefore, we recommend that future studies develop region-specific databases that incorporate the most relevant environmental drivers for each study area.

Another limitation of this study concerns the temporal scope of the analysis. We adopted a static framework, comparing a historical baseline (1970–2000) with a future projection period (2061−2080), whereas several previous studies have relied on dense historical time series to capture annual fluctuations in

NDVI (Pereira et al., 2024). Although annual time series provide valuable insights into short-term fluctuations and extreme events, a significant limitation persists in the availability of climate projections with comparable annual temporal resolution for future scenarios.

Additionally, the vegetation domains used in this study were based on the RADAMBRASIL project, with field surveys conducted between 1973 and 1982. We assume that these biomes will remain structurally comparable to the historical context. However, we recognize that changes in biome distribution are possible, such as xerification processes and forest-to-savanna transition (Oliveira et al., 2021). Therefore, we suggest that future studies analyze vegetation vigor considering its potential structural changes.

Despite these methodological constraints, the patterns identified in our study highlight important signals that demand urgent attention. The projected decline in vegetative vigor under future scenarios reinforces the need to strengthen conservation actions to safeguard the ecosystem services provided by the region's vegetation. Tropical forests (ombrophilous and seasonal) and the Caatinga, for instance, are essential for water regulation and carbon sequestration (Teixeira et al., 2023). In this context, proactive conservation planning becomes essential to maintain these ecosystem functions. Based on our projected vegetation vigor maps, areas of Caatinga and tropical forests identified as highly vulnerable to climate change could be prioritized in environmental zoning frameworks, especially those focused on ecological restoration and climate adaptation strategies.

In contrast, our projections indicate that the savannas of the Cerrado biome may show relative resilience under future climate change scenarios, with a significant gain in greenness levels. Based on these spatial projections, it is possible to identify priority areas for the expansion of conservation units in the Cerrado, especially with the aim of establishing climate refugia.

In this context, ecotonal zones, i.e., the transitional areas between major vegetation domains and recognized hotspots of high biodiversity, are particularly susceptible to increasing aridity under climate change (Smith and Goetz, 2021). Their vulnerability is further intensified by the lack of specific environmental protections in Brazil. In this context, our spatial projections enable the identification of climate-vulnerable ecotonal areas that could be prioritized for the establishment of conservation units and the implementation of ecological corridors to increase the ecological resilience of these transitional environments.

## 5. Final Considerations

In this study, we used the RF algorithm to evaluate the impacts of intensified aridification under future climate change scenarios on vegetation vigor in the BSR. Our model performed well, with a holdout test exhibiting an $R^2$ of 0.93. Additionally, the selected covariates explained 92% of the spatial variation in NDVI. Our results suggest that progressive aridification is likely to reduce vegetation vigor in the BSR by the end of the century. Consistent with regional trends, widespread browning pattern is projected for most of vegetation domains, except for savannas, which are expected to experience greening in the coming decades. These results emphasize the urgent need to strengthen public policies aimed at enhancing ecosystem resilience to climate change. Priority actions include: (i) expanding conservation units; (ii) establishing ecological corridors; and (iii) incorporating current and projected desertification zones into vegetation management and climate adaptation strategies. Such measures are critical for achieving the United Nations' Sustainable Development Goals.

## Author contributions: CRediT

**Lucas Augusto Pereira da Silva**: Writing – review & editing, Writing – original draft, Methodology, Investigation, Formal analysis, Conceptualization. **Cristiano Marcelo Pereira de Souza**: Writing – review & editing, Visualization. **Edson Eyji Sano**: Writing – review & editing. **Taya Cristo Parreiras**: Writing – review & editing. **Édson Luis Bolfe**: Writing – review & editing. **Bartolomeu Israel de Souza**: Writing – review & editing. **Ramon Santos Souza**: Writing – review & editing. **Marcos Esdras Leite**: Writing – review & editing. **Mário Marcos Espírito-Santo**: Writing – review & editing. **Carolina Cabral das Chagas-Reis**: Writing – review & editing. **Ivanildo Costa da Silva**: Writing – review & editing. **João Paulo**

**Sena-Souza**: Writing – review & editing. **Claudionor Ribeiro da Silva**: Writing – review & editing & Conceptualization.

## Funding sources

This work was supported by the Bahia State Research Support Foundation (FAPESB).

## References

Afshari, S., Sarli, R., Alchin, A.A., Aliabad, O.G., Moradi, F., Saei, M., Lomer, A.R.B., Nasiri, V., 2025. Trend analysis and interactions between surface temperature and vegetation condition: divergent responses across vegetation types. Environ. Monit. Assess. 197, 292. https://doi.org/10.1007/s10661-025-13729-9

Aguirre-Gutiérrez, J., Díaz, S., Rifai, S.W., Corral-Rivas, J.J., Nava-Miranda, M.G., González-M, R., Hurtado-M, A.B., Revilla, N.S., Vilanova, E., Almeida, E., de Oliveira, E.A., Alvarez-Davila, E., Alves, L.F., de Andrade, A.C.S., Lola da Costa, A.C., Vieira, S.A., Aragão, L., Arets, E., Aymard C., G.A., Baccaro, F., Bakker, Y.V., Baker, T.R., Bánki, O., Baraloto, C., de Camargo, P.B., Berenguer, E., Blanc, L., Bonal, D., Bongers, F., Bordin, K.M., Brienen, R., Brown, F., Prestes, N.C.C.S., Castilho, C.V., Ribeiro, S.C., de Souza, F.C., Comiskey, J.A., Valverde, F.C., Müller, S.C., da Costa Silva, R., do Vale, J.D., de Andrade Kamimura, V., de Oliveira Perdiz, R., del Aguila Pasquel, J., Derroire, G., Di Fiore, A., Disney, M., Farfan-Rios, W., Fauset, S., Feldpausch, T.R., Ramos, R.F., Llampazo, G.F., Martins, V.F., Fortunel, C., Cabrera, K.G., Barroso, J.G., Hérault, B., Herrera, R., Honorio Coronado, E.N., Huamantupa-Chuquimaco, I., Pipoly, J.J., Zanini, K.J., Jiménez, E., Joly, C.A., Kalamandeen, M., Klipel, J., Levesley, A., Oviedo, W.L., Magnusson, W.E., dos Santos, R.M., Marimon, B.S., Marimon-Junior, B.H., de Almeida Reis, S.M., Melo Cruz, O.A., Mendoza, A.M., Morandi, P., Muscarella, R., Nascimento, H., Neill, D.A., Menor, I.O., Palacios, W.A., Palacios-Ramos, S., Pallqui Camacho, N.C., Pardo, G., Pennington, R.T., de Oliveira Pereira, L., Pickavance, G., Picolotto, R.C., Pitman, N.C.A., Prieto, A., Quesada, C., Ramírez-Angulo, H., Réjou-Méchain, M., Correa, Z.R., Reyna Huaymacari, J.M., Rodriguez, C.R., Rivas-Torres, G., Roopsind, A., Rudas, A., Salgado Negret, B., van der Sande, M.T., Santana, F.D., Maës Santos, F.A., Bergamin, R.S., Silman, M.R., Silva, C., Espejo, J.S., Silveira, M., Souza, F.C., Sullivan, M.J.P., Swamy, V., Talbot, J., Terborgh, J.J., van der Meer, P.J., van der Heijden, G., van Ulft, B., Martinez, R.V., Vedovato, L., Vleminckx, J., Vos, V.A., Wortel, V., Zuidema, P.A., Zwerts, J.A., Laurance, S.G.W., Laurance, W.F., Chave, J., Dalling, J.W., Barlow, J., Poorter, L., Enquist, B.J., ter Steege, H., Phillips, O.L., Galbraith, D., Malhi, Y., 2025. Tropical forests in the Americas are changing too slowly to track climate change. Science 387, eadl5414. https://doi.org/10.1126/science.adl5414

Araújo Filho, J.C., Correa, M.M., Paiva, Arlicelio, Q., Costa, O.V., Valladares, G., Ribeiro, M.R., Carlos, E.G.R.S., 2023. Semi-arid soils of the Caatinga biome of Northeastern Brazil. In: The Soils of Brazil, World Soils Book Series. Springer International Publishing, Cham. https://doi.org/10.1007/978-3-031-19949-3

Borges, C.K., Carneiro, R.G., Santos, C.A., Zeri, M., Poczta, P., Cunha, A.P.M.A., Stachlewska, I.S., dos Santos, C.A.C., 2024. Partitioning of water vapor and $CO_2$ fluxes and underlying water use efficiency evaluation in a Brazilian seasonally dry tropical forest (Caatinga) using the Fluxpart model. J. S. Am. Earth Sci. 142, 104963. https://doi.org/10.1016/j.jsames.2024.104963

Brunson, J.C., 2020. Alluvial Plots in ggplot2.

Choat, B., Jansen, S., Brodribb, T.J., Cochard, H., Delzon, S., Bhaskar, R., Bucci, S.J., Feild, T.S., Gleason, S.M., Hacke, U.G., Jacobsen, A.L., Lens, F., Maherali, H., Martínez-Vilalta, J., Mayr, S., Mencuccini, M., Mitchell, P.J., Nardini, A., Pittermann, J., Pratt, R.B., Sperry, J.S., Westoby, M., Wright, I.J., Zanne, A.E., 2012. Global convergence in the vulnerability of forests to drought. Nature 491, 752–755. https://doi.org/10.1038/nature11688

Croitoru, A.-E., Piticar, A., Imbroane, A.M., Burada, D.C., 2013. Spatiotemporal distribution of aridity indices based on temperature and precipitation in the extra-Carpathian regions of Romania. Theor. Appl. Climatol. 112, 597–607. https://doi.org/10.1007/s00704-012-0755-2

D'Odorico, P., Bhattachan, A., Davis, K.F., Ravi, S., Runyan, C.W., 2013. Global desertification: drivers and feedbacks. Adv. Water Resour. 51, 326–344.

Dias, P.B., Horn Kunz, S., Pezzopane, J.E.M., Xavier, T.M.T., Zorzanelli, J.P.F., Toledo, J.V., Gomes, L.P., Gorsani, R.G., 2024. Water restriction alters seed bank traits and ecology in Atlantic Forest seasonal forests under climate change. Global Change Biology 30, e17494. https://doi.org/10.1111/gcb.17494

Dou, P., Wang, J., Cai, T., Miao, Z., Wang, X., Liang, J., Li, P., Fan, J., Tang, S., Xiao, X., Guo, L., Huang, J., Gao, Q., Chen, C., Liu, K., Wang, K., 2025. Influence of initial soil organic carbon in grassland on the sensitivity of carbon changes to climate after grassland-to-cropland conversion. Earth's Future 13, e2024EF005249. https://doi.org/10.1029/2024EF005249

Dunn, O.J., 1964. Multiple comparisons using rank sums. Technometrics 6, 241–252. https://doi.org/10.1080/00401706.1964.10490181

EMBRAPA, 2018. Sistema brasileiro de classificação de solos, 5th ed. Embrapa, Brasília, DF.

Fick, S.E., Hijmans, R.J., 2017. WorldClim 2: new 1-km spatial resolution climate surfaces for global land areas. Int. J. Climatol. 37, 4302–4315. https://doi.org/10.1002/joc.5086

Franca Rocha, W.J.S., Vasconcelos, R.N., Costa, D.P., Duverger, S.G., Lobão, J.S.B., Souza, D.T.M., Herrmann, S.M., Santos, N.A., Franca Rocha, R.O., Ferreira-Ferreira, J., Oliveira, M., Barbosa, L. da S., Cordeiro, C.L., Aguiar, W.M., 2024. Towards uncovering three decades of LULC in the Brazilian drylands: Caatinga biome dynamics (1985–2019). Land 13, 1250. https://doi.org/10.3390/land13081250

Greenwell, B., 2017. pdp: An R Package for Constructing Partial Dependence Plots. The R Journal.

Hamner, B., Frasco, M., 2012. Metrics: Evaluation metrics for machine learning. https://doi.org/10.32614/CRAN.package.Metrics

Hausfather, Z., Marvel, K., Schmidt, G.A., Nielsen-Gammon, J.W., Zelinka, M., 2022. Climate simulations: Recognize the 'hot model'problem.

Higgins, S.I., Conradi, T., Muhoko, E., 2023. Shifts in vegetation activity of terrestrial ecosystems attributable to climate trends. Nat. Geosci. 16, 147–153. https://doi.org/10.1038/s41561-022-01114-x

Hijmans, R.J., Van Etten, J., Cheng, J., Mattiuzzi, M., Sumner, M., Greenberg, J.A., Lamigueiro, O.P., Bevan, A., Racine, E.B., Shortridge, A., 2015. Package 'raster.' R package 734.

Huang, J., Zhang, G., Zhang, Y., Guan, X., Wei, Y., Guo, R., 2020. Global desertification vulnerability to climate change and human activities. Land Degrad. Dev. 31, 1380–1391.

IBGE, 2023. BDiA - Banco de Informações Ambientais [WWW Document]. URL https://www.ibge.gov.br/geociencias/informacoes-ambientais/vegetacao/23382-banco-de-informacoes-ambientais.html (accessed 2.27.25).

IPCC, 2021. Climate Change 2021 – The Physical Science Basis: Working Group I Contribution to the Sixth Assessment Report of the Intergovernmental Panel on Climate Change, 1st ed. Cambridge University Press. https://doi.org/10.1017/9781009157896

Jian, D., Niu, G.-Y., Ma, Z., Liu, H., Guan, D., Zhou, X., Zhou, J., 2023. Limited driving of elevated $CO_2$ on vegetation greening over global drylands. Environ. Res. Lett. 18, 104024. https://doi.org/10.1088/1748-9326/acf6d3

Kruskal, W.H., Wallis, W.A., 1952. Use of ranks in one-criterion variance analysis. J. Am. Stat. Assoc. 47, 583–621. https://doi.org/10.1080/01621459.1952.10483441

Kuhn, M., Wing, J., Weston, S., Williams, A., Keefer, C., Engelhardt, A., Cooper, T., Mayer, Z., Kenkel, B., Team, R.C., 2020. Package 'caret.' The R Journal 223, 7.

Liaw, A., Wiener, M., 2002. Classification and regression by randomForest. R news 2, 18–22.

Liu, B., Sun, J., Liu, M., Zeng, T., Zhu, J., 2019. The aridity index governs the variation of vegetation characteristics in alpine grassland, Northern Tibet Plateau. PeerJ 7, e7272. https://doi.org/10.7717/peerj.7272

Liu, Y., Liu, H., Chen, Y., Gang, C., Shen, Y., 2022. Quantifying the contributions of climate change and human activities to vegetation dynamic in China based on multiple indices. Sci. Total Environ. 838, 156553. https://doi.org/10.1016/j.scitotenv.2022.156553

Lu, C., Zhang, Q., Woolway, R.I., Ma, L., Liu, T., Wang, G., Sun, D., Singh, V.P., Bai, Y., Sun, B., Huang, X., 2025. Global warming will increase the risk of water shortage in Northwest China. Earth's Future 13, e2025EF006199. https://doi.org/10.1029/2025EF006199

Ma, C., Li, T., Liu, P., 2021. GIMMS NDVI3g+ (1982–2015) response to climate change and engineering activities along the Qinghai–Tibet Railway. Ecological Indicators 128, 107821. https://doi.org/10.1016/j.ecolind.2021.107821

Ma, N., Cao, S., Bai, T., Yang, Z., Cai, Z., Sun, W., 2025. Assessment of vegetation dynamics in Xinjiang using NDVI data and machine learning models from 2000 to 2023. Sustainability 17, 306. https://doi.org/10.3390/su17010306

Mapbiomas. MapBiomas Project of the Annual Land Use and Land Cover Maps of Brazil. 2023. Available online: https://brasil.mapbiomas.org/ (accessed on 5 February 2026).

Moro, M.F., Amorim, V.O., de Queiroz, L.P., da Costa, L.R.F., Maia, R.P., Taylor, N.P., Zappi, D.C., 2024. Biogeographical Districts of the Caatinga Dominion: A proposal based on geomorphology and endemism. Bot. Rev. 90, 376–429. https://doi.org/10.1007/s12229-024-09304-5

Nguyen, K.A., Seeboonruang, U., Chen, W., 2023. Projected climate change effects on global vegetation growth: A machine learning approach. Environments 10, 204. https://doi.org/10.3390/environments10120204

Nyamtseren, M., Feng, Q., Deo, R.C., 2018. A comparative study of temperature and precipitation-based aridity indices and their trends in Mongolia. Int. J. Environ. Res. 12, 887–899. https://doi.org/10.1007/s41742-018-0143-6

Ogle, D.H., Doll, J.C., Wheeler, A.P., dunnTest()), A.D. (Provided base functionality of, 2023. FSA: Simple Fisheries Stock Assessment Methods.

Oliveira, A.C.P., Nunes, A., Oliveira, M.A., Rodrigues, R.G., Branquinho, C., 2022. How do taxonomic and functional diversity metrics change along an aridity gradient in a tropical dry forest? Front Plant Sci. 13, 923219. https://doi.org/10.3389/fpls.2022.923219

Oliveira, G. de C., Arruda, D.M., Fernandes Filho, E.I., Veloso, G.V., Francelino, M.R., Schaefer, C.E.G.R., 2021. Soil predictors are crucial for modelling vegetation distribution and its responses to climate change. Sci. Total Environ. 780, 146680. https://doi.org/10.1016/j.scitotenv.2021.146680

Oyama, M.D., Nobre, C.A., 2004. Climatic consequences of a large-scale desertification in Northeast Brazil: A GCM simulation study. J. Climate 17, 3203–3213. https://doi.org/10.1175/1520-0442(2004)017<3203:CCOALD>2.0.CO;2

Pereira, L.F., Fernandes-Filho, E.I., Gomes, L.C., Arruda, D.M., Oliveira, G.C., Schaefer, C.E.G.R., de Souza, J.J.L.L., Francelino, M.R., 2024. Soil and vegetation types are predisposition factors controlling greenness changes: A shift of paradigm in greening and browning modelling? Remote Sens. Appl. Soc. Environ. 36, 101366. https://doi.org/10.1016/j.rsase.2024.101366

Piao, S., Wang, X., Park, T., Chen, C., Lian, X., He, Y., Bjerke, J.W., Chen, A., Ciais, P., Tømmervik, H., Nemani, R.R., Myneni, R.B., 2020. Characteristics, drivers and feedbacks of global greening. Nat. Rev. Earth Environ. 1, 14–27. https://doi.org/10.1038/s43017-019-0001-x

Pinto, A.S., Monteiro, F.K. da S., Rodrigues, E. de M., Gomes, D.R.F.L., Medeiros, M.C., Lopes, S. de F., 2025. Phylogenetic diversity and conservation challenges in Brejos de Altitude: assessing threatened areas of the Brazilian Atlantic Forest. Reg. Environ. Change 25, 15. https://doi.org/10.1007/s10113-024-02353-x

Poggio, L., Sousa, L.M.D., Batjes, N.H., Heuvelink, G.B.M., Kempen, B., Ribeiro, E., Rossiter, D., 2021. SoilGrids 2.0: Producing soil information for the globe with quantified spatial uncertainty. Soil 7, 217–240. https://doi.org/10.5194/soil-7-217-2021

Quan, C., Han, S., Utescher, T., Zhang, C., Liu, Y.-S.C., 2013. Validation of temperature–precipitation based aridity index: paleoclimatic implications. Palaeogeogr. Palaeoclimatol. Palaeoecol. 386, 86–95. https://doi.org/10.1016/j.palaeo.2013.05.008

Ramos, M.B., Diniz, F.C., Almeida, H.A. de, Almeida, G.R. de, Pinto, A.S., Meave, J.A., Lopes, S. de F., 2020. The role of edaphic factors on plant species richness and diversity along altitudinal gradients in the Brazilian semi-arid region. J. Trop. Ecol. 36, 199–212. https://doi.org/10.1017/S0266467420000115

Reboita, M.S., Rodrigues, M., Armando, R., Freitas, C., Martins, D., Miller, G., 2016. Causas da semi-aridez do Sertão Nordestino. Rev. Bras. Climatol. 19, 254-277. https://doi.org/10.5380/abclima.v19i0.42091

Ribeiro, J.F., Walter, B.M.T., 2008. Fitofisionomias do bioma Cerrado. pp. 152-212. In: S.M. Sano; S.P. Almeida; J.F. Ribeiro (eds.). Cerrado: Ecologia e Flora, Planaltina, DF: Embrapa Cerrados.

Robbins, Z., Chambers, J., Chitra-Tarak, R., Christoffersen, B., Dickman, L.T., Fisher, R., Jonko, A., Knox, R., Koven, C., Kueppers, L., McDowell, N., Xu, C., 2024. Future climate doubles the risk of hydraulic failure in a wet tropical forest. New Phytologist 244, 2239–2250. https://doi.org/10.1111/nph.19956

Santos, J.C., Leal, I.R., Almeida-Cortez, J.S., Fernandes, G.W., Tabarelli, M., 2011. Caatinga: The scientific negligence experienced by a dry tropical forest. Trop. Conserv. Sci. 4, 276–286. https://doi.org/10.1177/194008291100400306

Scheiter, S., Higgins, S.I., 2009. Impacts of climate change on the vegetation of Africa: an adaptive dynamic vegetation modelling approach. Glob. Change Biol. 15, 2224–2246. https://doi.org/10.1111/j.1365-2486.2008.01838.x

Smith, A.J., Goetz, E.M., 2021. Climate change drives increased directional movement of landscape ecotones. Landscape Ecol. 36, 3105–3116. https://doi.org/10.1007/s10980-021-01314-7

Stan, K.D., Sanchez-Azofeifa, A., Duran, S.M., Guzman Q, J.A., Hesketh, M., Laakso, K., Portillo-Quintero, C., Rankine, C., Doetterl, S., 2021. Tropical dry forest resilience and water use efficiency: an analysis of productivity under climate change. Environ. Res. Lett. 16, 054027. https://doi.org/10.1088/1748-9326/abf6f3

Stan, K.D., Sanchez-Azofeifa, A., Hamann, H.F., 2024. Widespread degradation and limited protection of forests in global tropical dry ecosystems. Biological Conservation 289, 110425. https://doi.org/10.1016/j.biocon.2023.110425

Teixeira, A., Leivas, J., Takemura, C., Bayma, G., Garçon, E., Sousa, I., Farias, F., Silva, C., 2023. Remote sensing environmental indicators for monitoring spatial and temporal dynamics of weather and vegetation conditions: applications for Brazilian biomes. Environ. Monit. Assess. 195, 944. https://doi.org/10.1007/s10661-023-11560-8

Teng, H., Chen, S., Hu, B., Shi, Z., 2023. Future changes and driving factors of global peak vegetation growth based on CMIP6 simulations. Ecological Informatics 75, 102031. https://doi.org/10.1016/j.ecoinf.2023.102031

Tisdall, J.M., Oades, J.M., 1982. Organic matter and water-stable aggregates in soils. Journal of Soil Science 33, 141–163. https://doi.org/10.1111/j.1365-2389.1982.tb01755.x

Tomasella, J., do Amaral Cunha, A.P.M., Zeri, M., Costa, L.C.O., 2025. Changes in the aridity index across Brazilian biomes. Sci. Total Environ. 989, 179869. https://doi.org/10.1016/j.scitotenv.2025.179869

van Zyl, J.J., 2001. The Shuttle Radar Topography Mission (SRTM): a breakthrough in remote sensing of topography. Acta Astronautica 48, 559–565.

Vieira, R. da S.P., Tomasella, J., Alvalá, R., Sestini, M., Affonso, A., Rodriguez, D., Barbosa, A., Cunha, A., Valles, G., Crepani, E., 2015. Identifying areas susceptible to desertification in the Brazilian northeast. Solid Earth 6, 347–360.

Yang, Y., Yin, J., Slater, L.J., Liu, P., Zhang, L., Zhang, Y., 2025. Global vegetation dynamics under decreased terrestrial water storage: Insights into water stress response. Agric. For. Meteorol. 368, 110549. https://doi.org/10.1016/j.agrformet.2025.110549

Zhang, X., Evans, J.P., Burrell, A.L., 2024. Less than 4% of dryland areas are projected to desertify despite increased aridity under climate change. Commun. Earth Environ. 5, 1–9. https://doi.org/10.1038/s43247-024-01463-y

## Ethics in Publishing Statement

I testify on behalf of all co-authors that our article submitted followed ethical principles in publishing.

Title: Climate change-driven aridity threatens vegetation vigor in Brazilian semiarid region

All authors agree that:

This research presents an accurate account of the work performed, all data presented are accurate and methodologies detailed enough to permit others to replicate the work.

This manuscript represents entirely original works and or if work and/or words of others have been used, that this has been appropriately cited or quoted and permission has been obtained where necessary.

This material has not been published in whole or in part elsewhere.

The manuscript is not currently being considered for publication in another journal.

That generative AI and AI-assisted technologies have not been utilized in the writing process or if used, disclosed in the manuscript the use of AI and AI-assisted technologies and a statement will appear in the published work.

That generative AI and AI-assisted technologies have not been used to create or alter images unless specifically used as part of the research design where such use must be described in a reproducible manner in the methods section.

All authors have been personally and actively involved in substantive work leading to the manuscript and will hold themselves jointly and individually responsible for its content.

Corresponding author's name: Lucas Augusto Pereira da Silva

Date: 22/10/2025

**Declaration of interests**

☒ The authors declare that they have no known competing financial interests or personal relationships that could have appeared to influence the work reported in this paper.

☐ The authors declare the following financial interests/personal relationships which may be considered as potential competing interests: